(9) Progress Report No. 3
1 Oct - 31 Dec 65
for the Period

October 1 to December 31, 1965

(6) THE EFFECT OF METAL PROPERTIES
ON
HYPERVELOCITY PENETRATION

(15) Contract No. DA 18-001-AMC-745(x)
with
Aberdeen Proving Ground

by

(10) Robert E. Green, Jr., Principal Investigator
(11) 31 Dec 65,
The Johns Hopkins University
Baltimore, Maryland

(12) 21p

191750

(8)

Ord 3

Analysis of the terminal displacement fields of five wire-mesh copper targets (described in a previous report, No. 11, DA 36-034-ORD-3565RD) fired at hypervelocity was carried out. These displacements were used to compute Lagrangian strains presuming cylindrically symmetric flow patterns. The second invariant of the strain tensor was calculated and compared to hardness profiles taken on the targets. A sixth specimen was impressed statically and observations on its displacement field are compared with the dynamic case.

Regions of material flow were observed qualitatively and are described by the following terms: a) evacuated volume; b) reverse flow to form the lip; and, c) region of approximate spherical symmetry.

Finally, problems encountered and suggestions for further work are included at the end of this report.

In order to document the strain and displacement fields occurring in targets fired at hypervelocity, five copper targets were formed from rectangular plates nominally 3/8" x 3" x 3". Prior to joining eight such plates to give a target 3" x 3" x 3", shallow grooves were machined in these plates and .005" nickel wire was placed in the grooves (see Fig. 1a). After joining the plates by one of the two techniques described below, the targets contained six parallel planes of two dimensional arrays of wires (see Fig. 1b). The wires in any plane intersect to form squares of sides 3/8".

After firing, the target was sectioned through the crater center so that the section was perpendicular to the initial direction of one of the sets of wires which formed the planar arrays. Subsequent lathe cuts (incremental) parallel to this face permit documentation of the terminal position of this set of wires. In general, only one set of wires in the planar array gives information by this section technique. It is necessary to have two forming the orthogonal network in order to have a choice of section direction after firing. The terminal positions of the wires are measured using a cathetometer. The accuracy of the measurements is $\pm$ .005 cm. The lathe cuts remained within 0.02 in. parallel to the rear surface (opposite to section plane, not impact direction). The origin of the coordinates was chosen to be a corner of the target sufficiently removed from the crater to be undeformed.

The plates were joined to form targets by one of two techniques:

A. A diffusion welding technique previously described in Progress Report No. 11, Contract No. DA-36-034-ORD-3565RD. This technique introduced a copper-copper oxide interface between the plates.

B. Silver solder technique:

The plates were machined as in A. to 3/8" x 3" x 3" and shallow parallel grooves of 3/8" spacing milled into them. The plates were wound with wire and stacked to form an orthogonal net. The silver solder sheets placed between the plates formed the bond. Stacks were compressed to 100,000 psi in steel clasps. Then the ensemble was placed in a furnace at 1400°F, allowed to reach temperature and held for 30 min. After this they were air cooled.

In either case A or B, the targets were then machined to cubic form; and, after etching the target, the initial wire positions were delineated on the four lateral faces.

Obviously, both joining techniques introduce interfaces which may affect the response of the targets to the impact. The use of two joining techniques allows an examination of the effect of the bond. The axis of impact relative to the stacking of the plates was varied and the thickness of the plate containing the impact surface was varied also.

The table below gives some qualitative information about the response of the target as affected by the aforementioned parameters.

Table I

Tgt. No.	V_I f.p.s.	E_I (Joules)	Bond	V_c (cm^3)	Axis of Impact
S1	10,470	2232	Cu-CuO	1.355	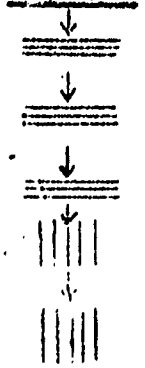
S2	10,580	2285	Silver solder	1.373	
S3	10,225	2142	Cu-CuO	2.537	
S4	10,320	2175	Silver-solder	1.443	
S5	12,575	3234	Cu-CuO	1.540	

Remarks:

1. S1 and S2 have displacement fields both qualitatively and quantitatively similar.
2. In S3 the top plate was milled to 3/16" nominal thickness. This plate split from the rest of the target upon firing and was bent to a convex shape with respect to the axis of the striking projectile. Only the top plate was penetrated. The vertical displacement (position "down" or negative "up") were larger than that in S1 or S2.
3. S4 has smaller vertical displacements than those in S1 or S2 for the same initial distance from the impact center.
4. Target S5 split along an interface at the center of the crater. Its displacement field is greater in magnitude than those of targets which did not split. However, S5 had a higher impact energy.
5. Target S6 was impressed statically with a steel ball, the impression being 80% of the volume of craters in S1 and S2. The displacement field was of larger magnitude at the same

distances from the surface and extended farther into the target than in S1 or S2. The total work done in this case was 50 Joules. No lip was formed in this annealed "target." In fact, there is a general sinking of material as the indentation was approached.

These results (1. through 5.) are readily seen from displacement plots at the end of this report.

We make the following generalization: The effect of changing the orientation of the plates is greater than the effect of changing the type of bond so long as splitting does not occur. It is felt that the results for S3 indicate a reflection phenomenon of either a tensile release wave from the free surface or a reflected compression wave from the interface. Another possibility of interpretation is bending due to inertia forces in the flow of material to form the lip.

From the split targets S5 and S3 it was possible to ascribe a maximum volume for the ejected material relative to the undeformed target. This volume if assumed hemispherical is less than 30% of the terminal crater volume. This figure agrees quite well with the BRL mass loss measurements on 2S Al, 2024 Al and tough pitch Cu targets (see Progress Report No. 1).

Derivation of the Eulerian and Lagrangian Displacement Fields:

Throughout this paper capital letters will designate Lagrangian variables, lower case letters will designate Eulerian variables. The Lagrangian displacement field is given by displacement of points versus the initial position of the points. The Eulerian displacement field is given by plots of displacement versus terminal positions.

The measurement of terminal wire positions were plotted for constant cross sections (Fig. 5a). The target free surfaces were assumed undeformed and the initial wire positions were superposed on these plots. Results typical of a section are shown (Fig. 5b).

Consideration of the data indicates that one must make some assumption about the symmetry character of the displacement field in order to determine from what initial position points on the terminal line came. Hardness contours and displacement plots indicate that an axis of symmetry passes through the center of the crater perpendicular to the impact surface. The subsequent choice of the coordinate system is shown (Fig. 7).

On the assumption of cylindrical symmetry, displacements in the R directions are duplicated in the x directions; it is then possible to compute or to measure (with dividers) the initial position and displacement from plots such as 5b. The displacements in the Z direction are designated W. The displacements in the R direction are designated v. Plots in figures (6, 3, 4) give vector displacement from initial position, displacement versus initial position and displacement versus final position. Before calculating

the finite Lagrangian strains we shall discuss some approximations and the general character of the flow field.

Adjacent to the crater surface is a region of reverse flow to form the lip. Wires are observed extending into the lip. In 2S Al targets macroetched as fired, grain elongation along the crater wall shows that considerable plastic flow is associated with a region approximately as wide as the maximum lip width. This region has a maximum width of .4 cm in the targets examined. The ejecta volume which has been discussed previously is depicted in Fig. 8 also. A large region of the target (shown in Fig. 8) has an approximately radial displacement field. Displacements calculated under this assumption are plotted in Figs. 9-10 and an equation is fitted to the data.

Calculations of finite Lagrangian strain have been made (it is not possible to approximate the derivations for the Eulerian strains). Once the Lagrangian strain tensor is derived, its second invariant is calculated and plotted in a terminal configuration (Fig. 11). It was originally felt that this invariant should be related to the energy absorbed and hence to hardness profiles taken on the targets. Such hardness profiles were made (Fig. 12) and were compared with the contour plot of the calculated second invariant. However, it is now felt that the energy absorbed (or the hardness level) is more likely some function of all three invariants of the strain tensor.

In the course of this work we have demonstrated the ability to perform measurements to document the terminal displacement field. We have discovered certain aspects of this field in regions removed

from the crater. An ejecta volume has been identified which correlates with previous data in the field. A region of reversed flow to form the lip has been identified. The orientation of the interfaces relative to the axis of impact has been observed to affect the character of the deformation field.

Problems:

1. The initial grid size in these targets was such that only two or, at most, four wires were close enough to the crater to yield much information.
2. Only one wire (in S5) was actually in the shear flow region adjacent to the crater.
3. The difference between macroscopic and microscopic strains -- points observed to undergo small displacements have relatively high hardness levels. This technique may not adapt itself to direct measurement of dilatational strains (where small strains may correspond to very high energy absorption).
4. The reaction of a particle of material first being pushed and then pulled (redundant work) will not appear in this terminal documentation.

Suggestions:

1. Targets containing a finer mesh will be fired in order to document flow near the crater.
2. The relation between hardness and the strain invariants will be investigated.
3. Higher energy targets will lead to a search for similarity in the flow field below the crater, i.e. we hope to answer the question of how this flow field changes with velocity or crater size/shape energy, etc.

Fig. 1a

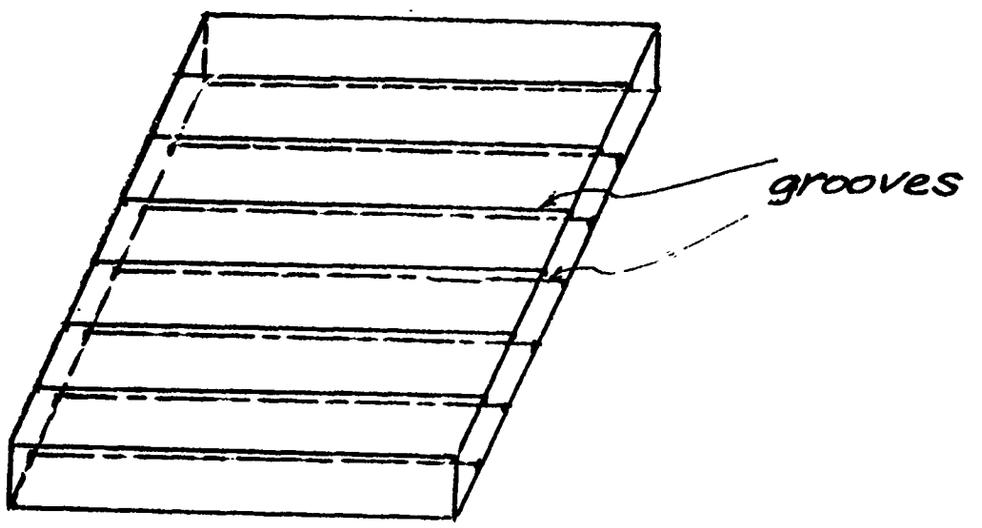

Fig. 1b

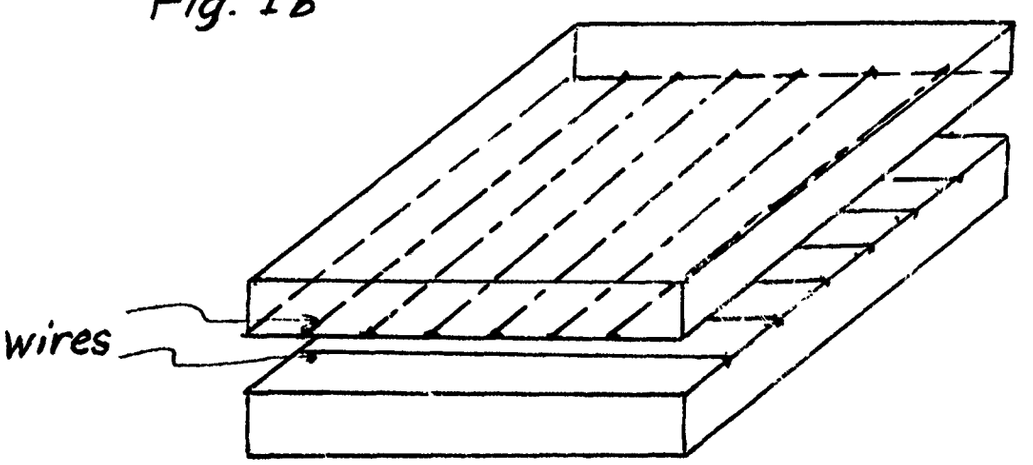

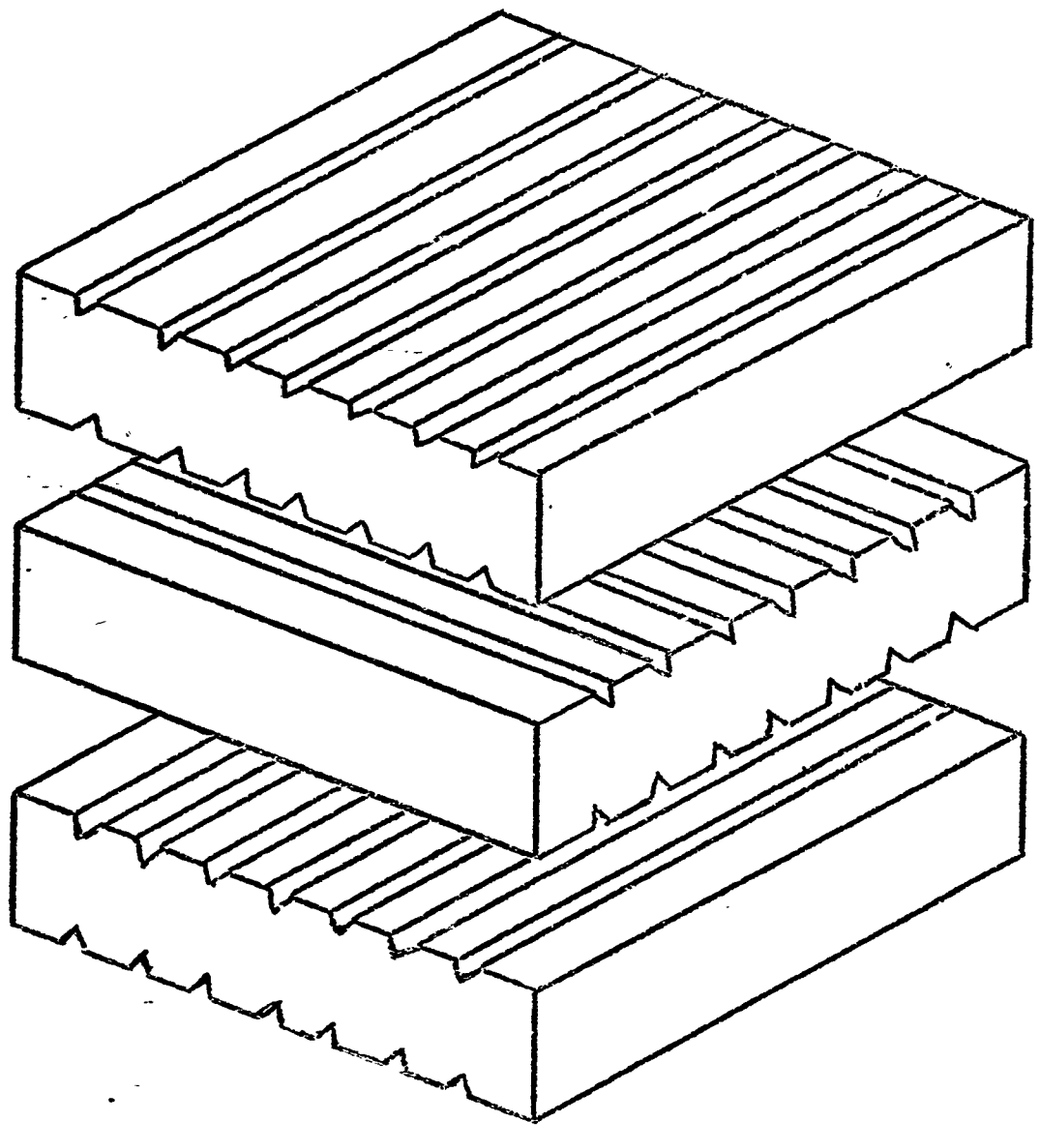

FIGURE 2. ILLUSTRATION OF STACKING OF TARGET SEGMENTS

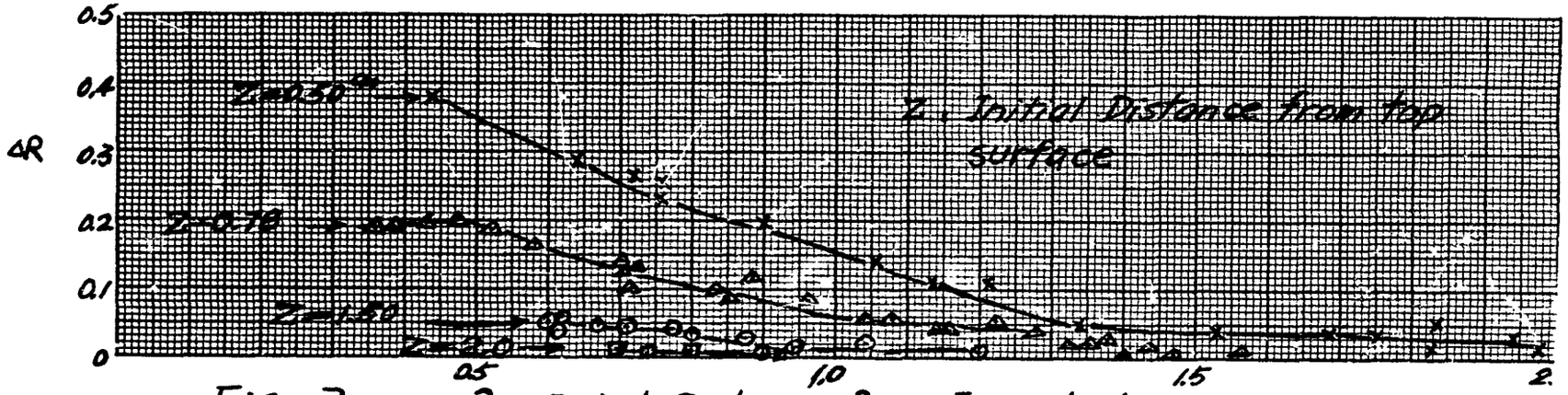

Fig. 3 R Initial Distance from Impact Axis (cm)

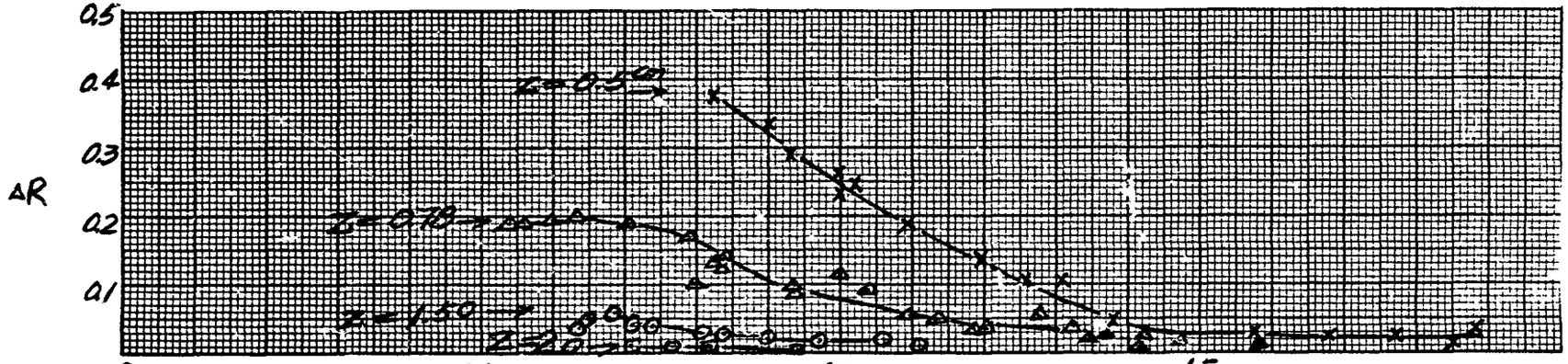

Fig. 4 a r Final Distance from Impact Axis (cm)

Fig. 4b

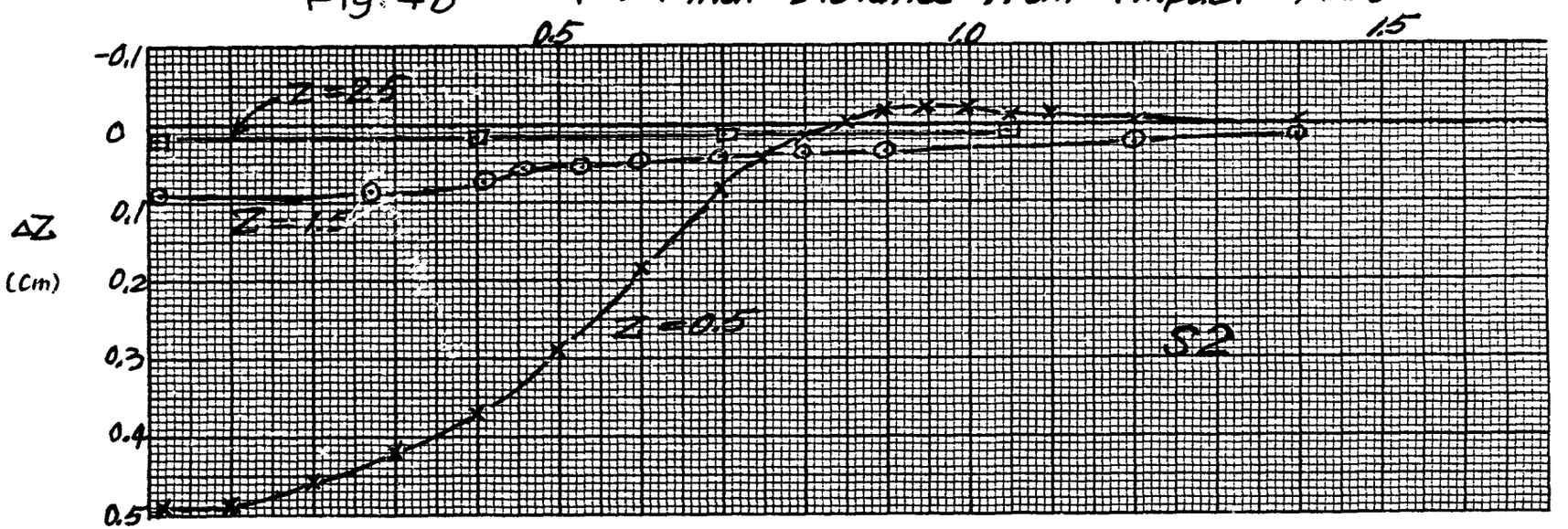
r : Final Distance from Impact Axis (cm)
0.5
1.0
1.5
-0.1
0
0.1
0.2
0.3
0.4
0.5
ΔZ
(cm)
Z = 2.5
Z = 1.5
Z = 0.5
52

Fig. 5a.

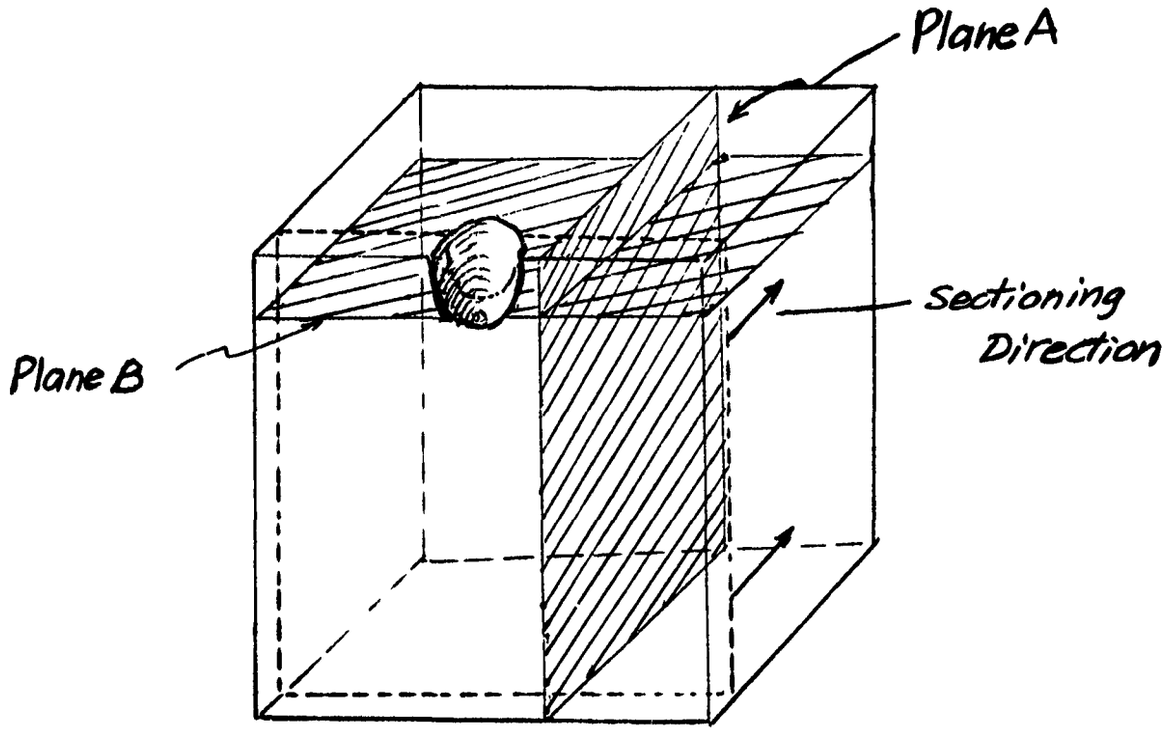
Plane A
Plane B
Sectioning Direction

Fig. 5b

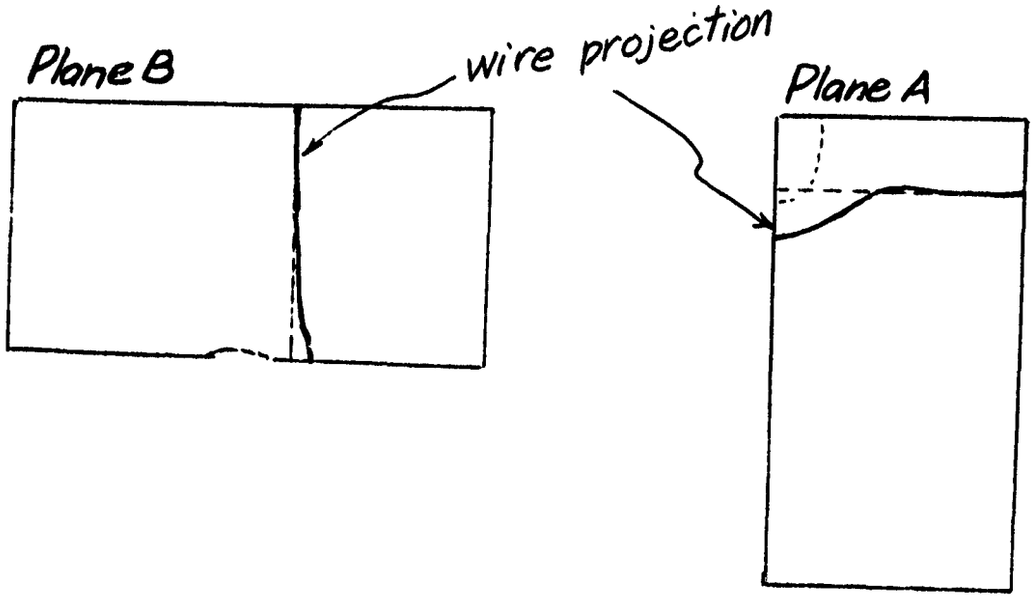
Plane B
wire projection
Plane A

Fig. 6 a

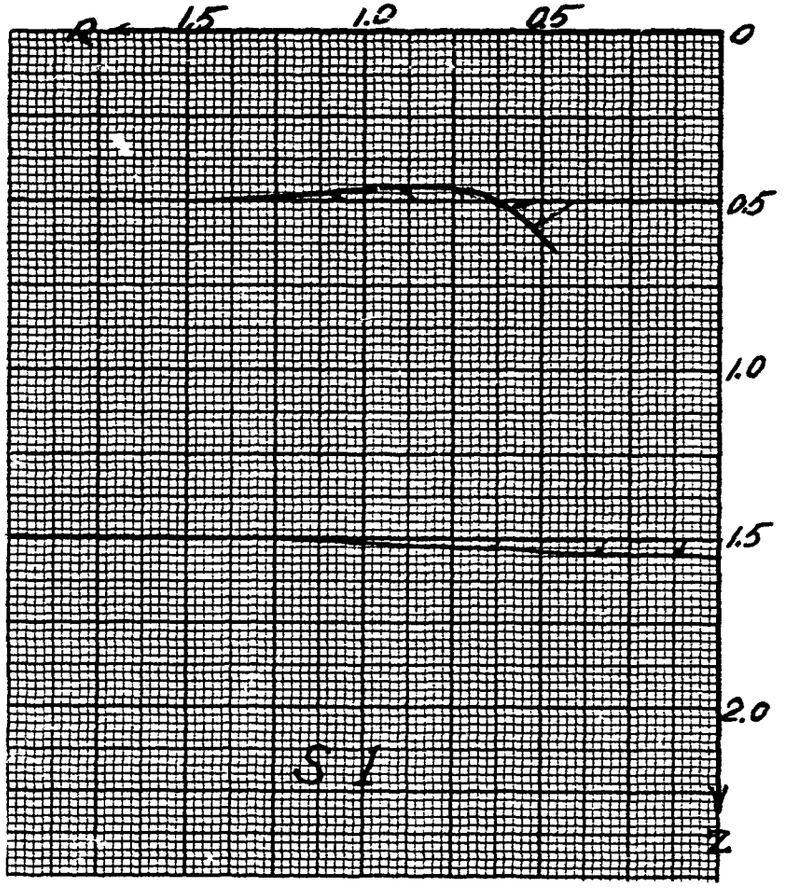

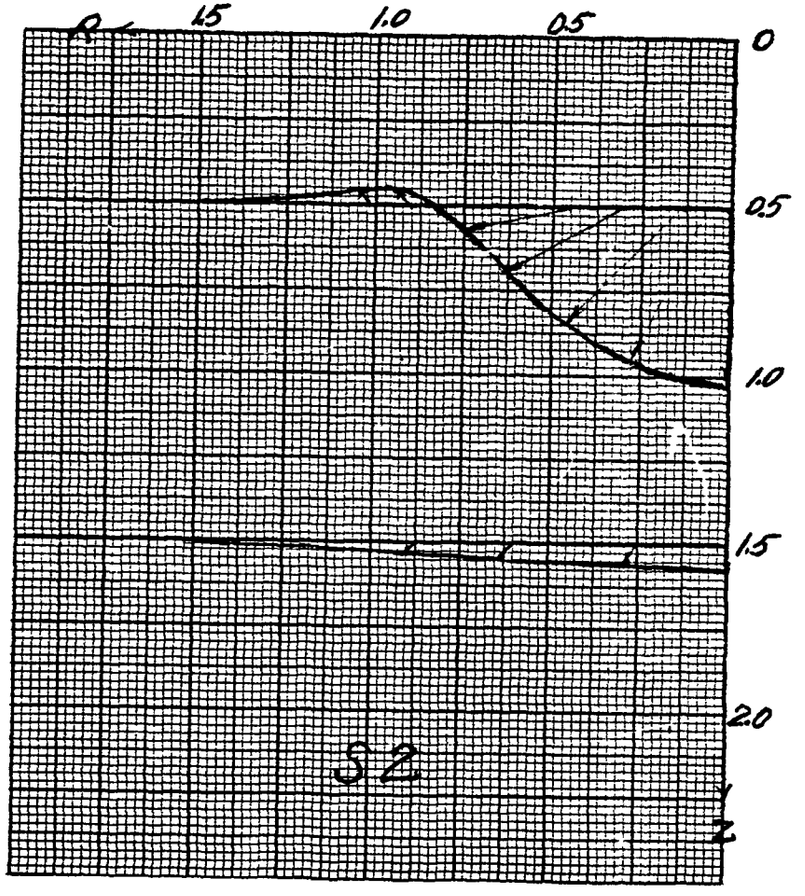

Fig. 6b

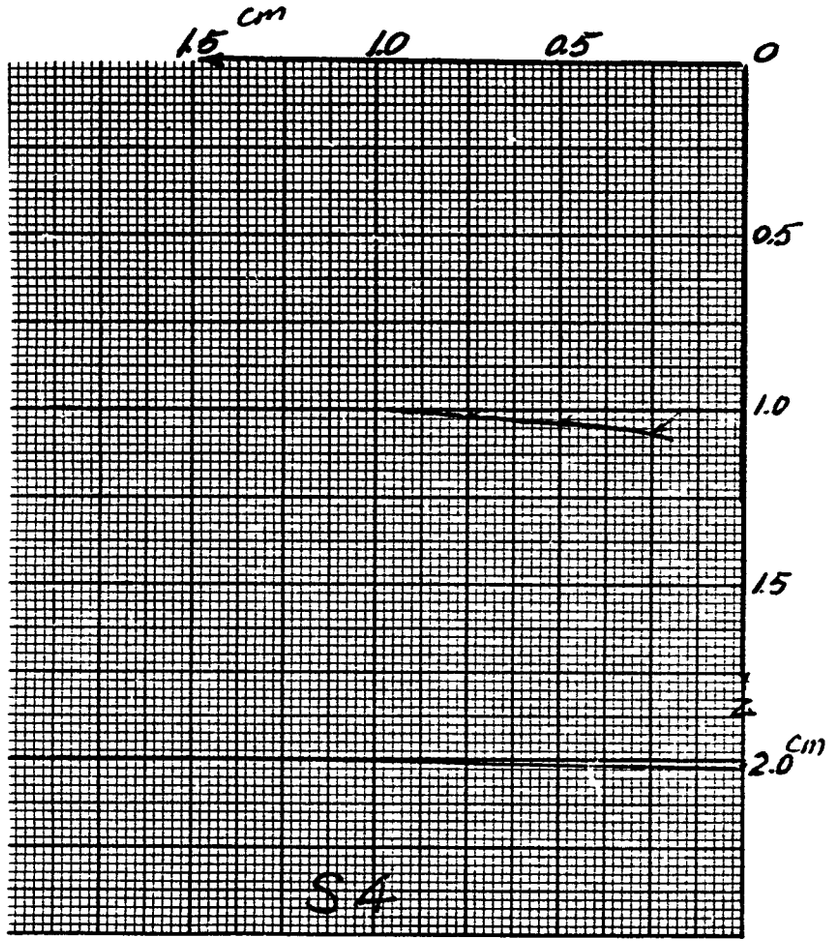

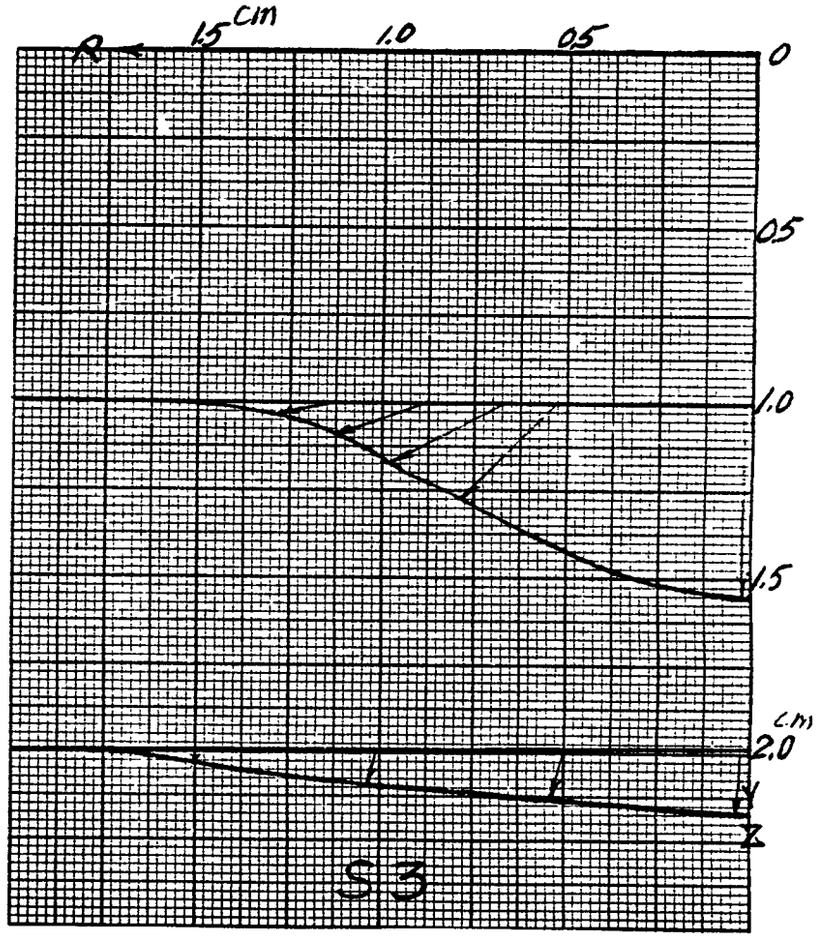

Fig. 6c

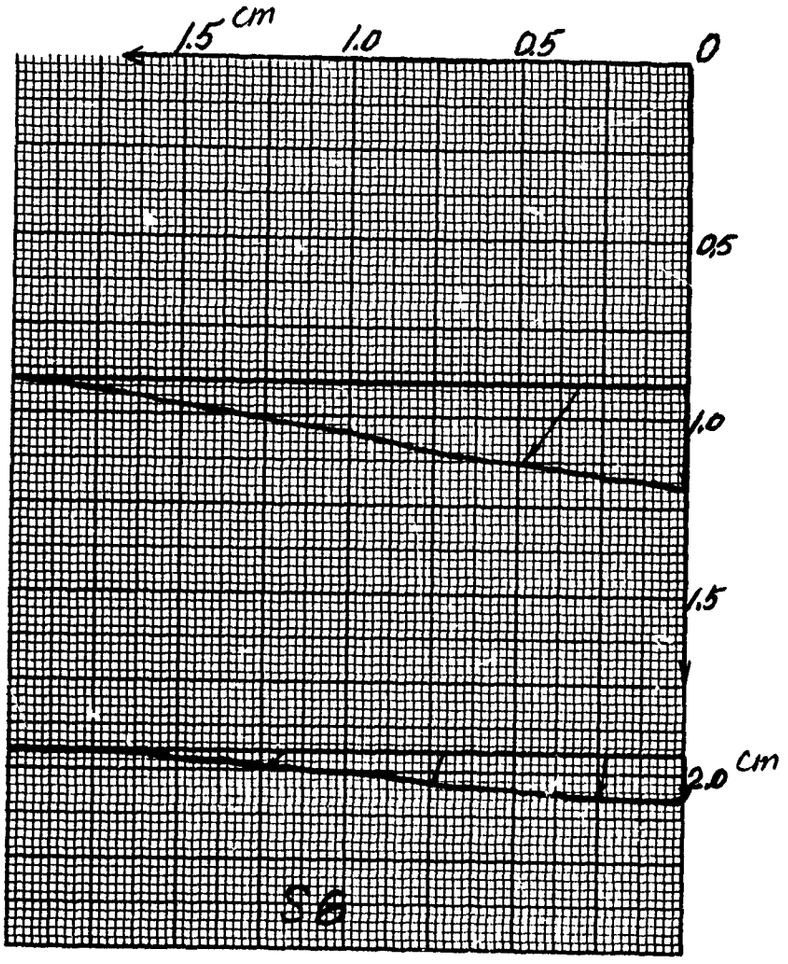

Fig. 7

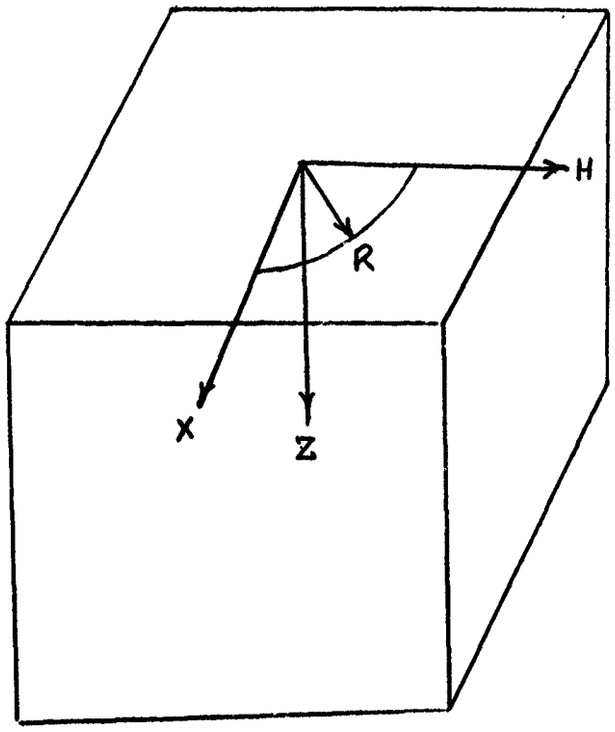
H
R
X
Z

Fig. 8

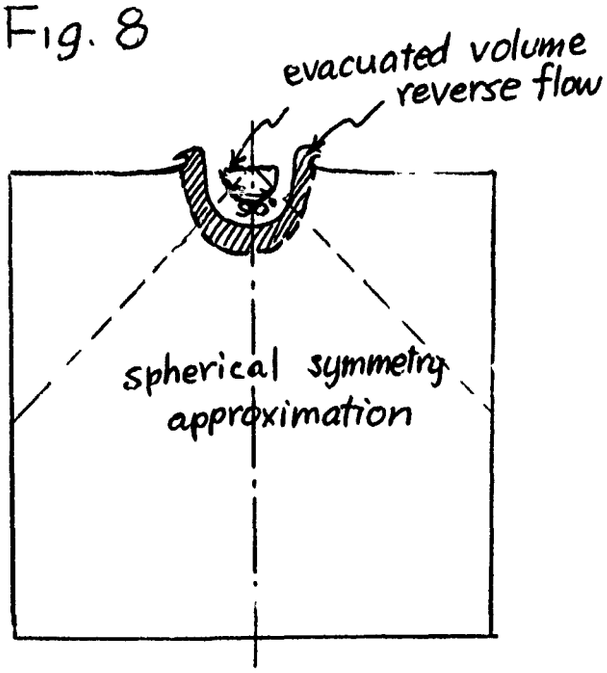
evacuated volume
reverse flow
spherical symmetry
approximation

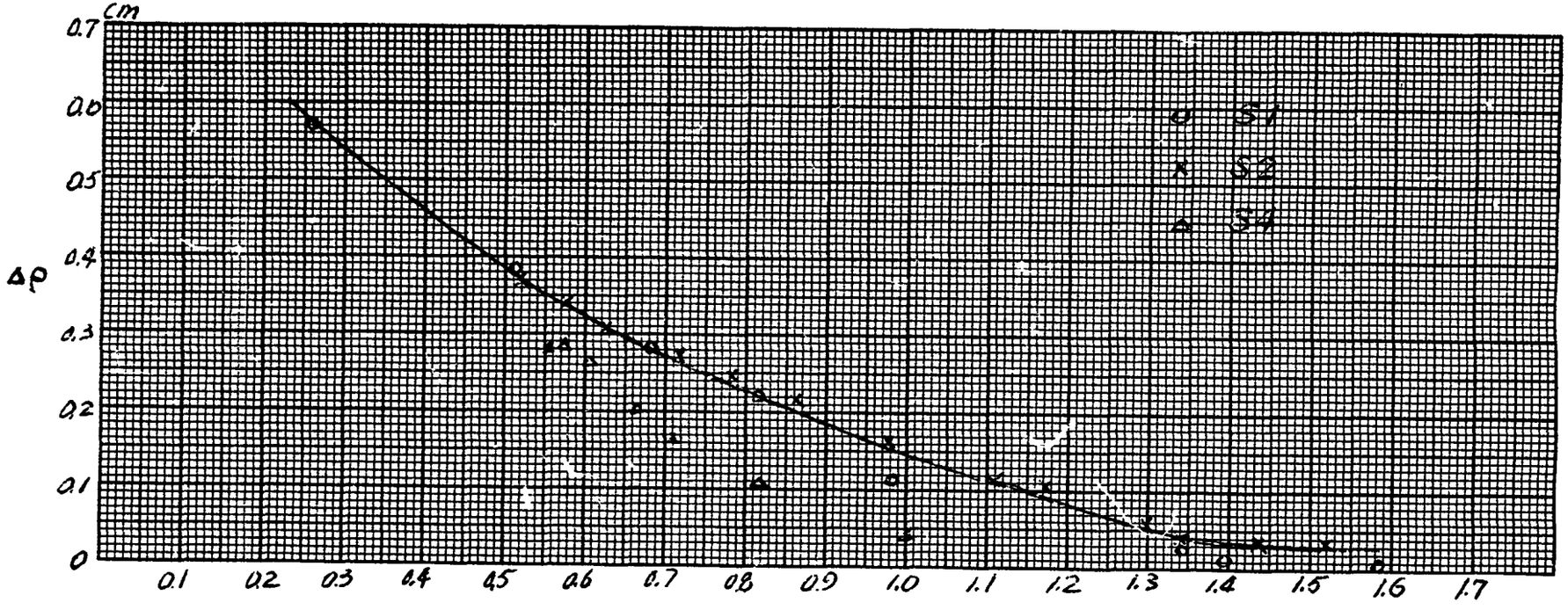

Fig. 9 ρ Initial Distance from Impact center (cm)

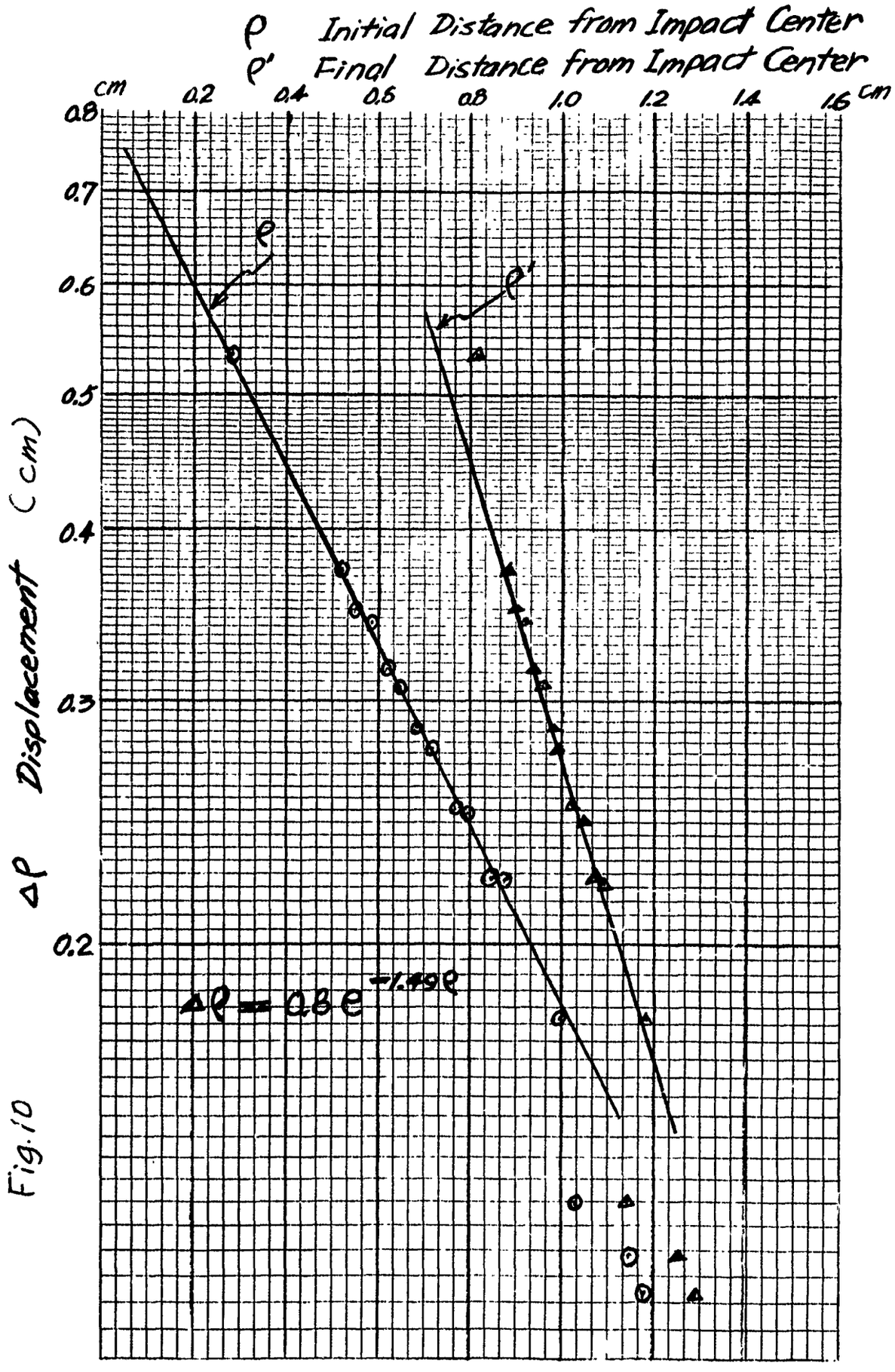
ρ Initial Distance from Impact Center
ρ' Final Distance from Impact Center
cm
0.2
0.4
0.6
0.8
1.0
1.2
1.4
1.6 cm
0.8
0.7
0.6
0.5
0.4
0.3
0.2
ρ
ρ'
Δρ Displacement (cm)
Δρ = 0.8 e^-1.49ρ

Fig. 10

Fig. 11 Second Invariant Field

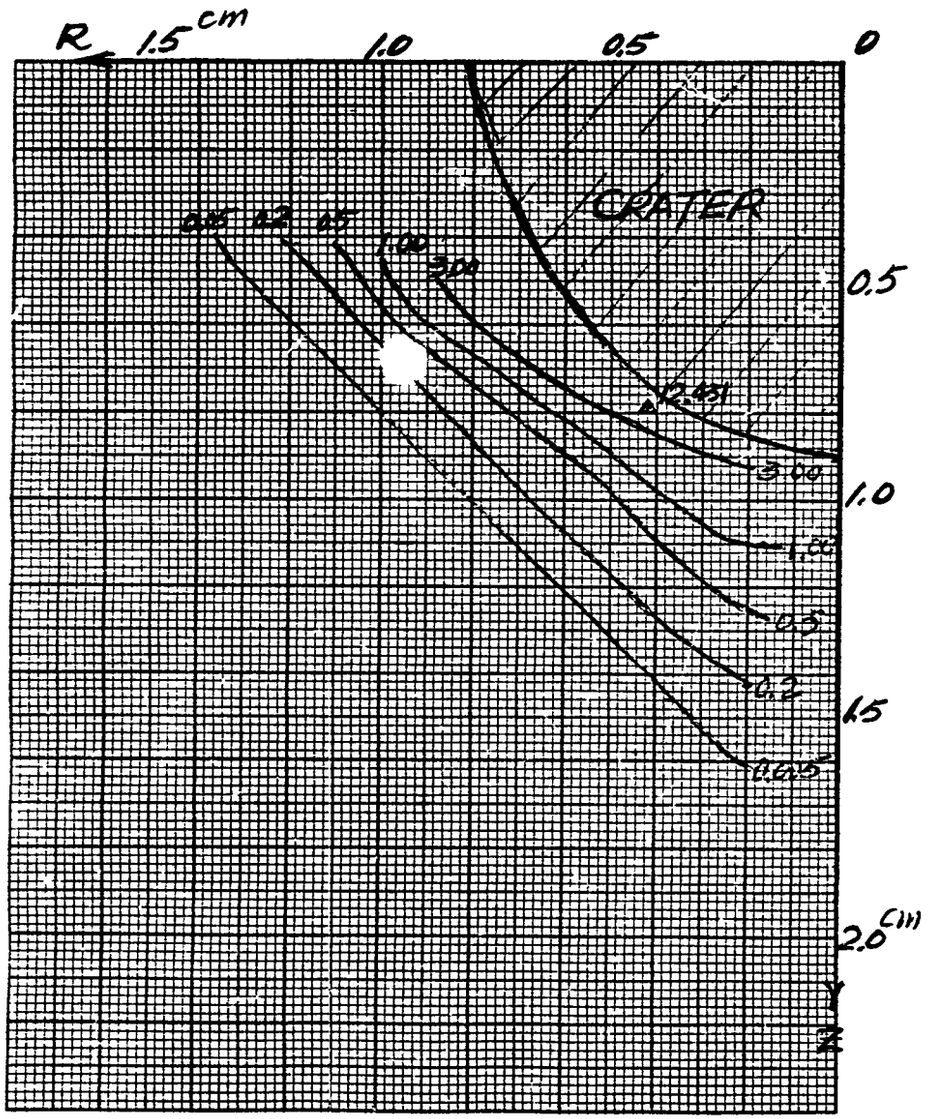

Fig. 12 Hardness Profile

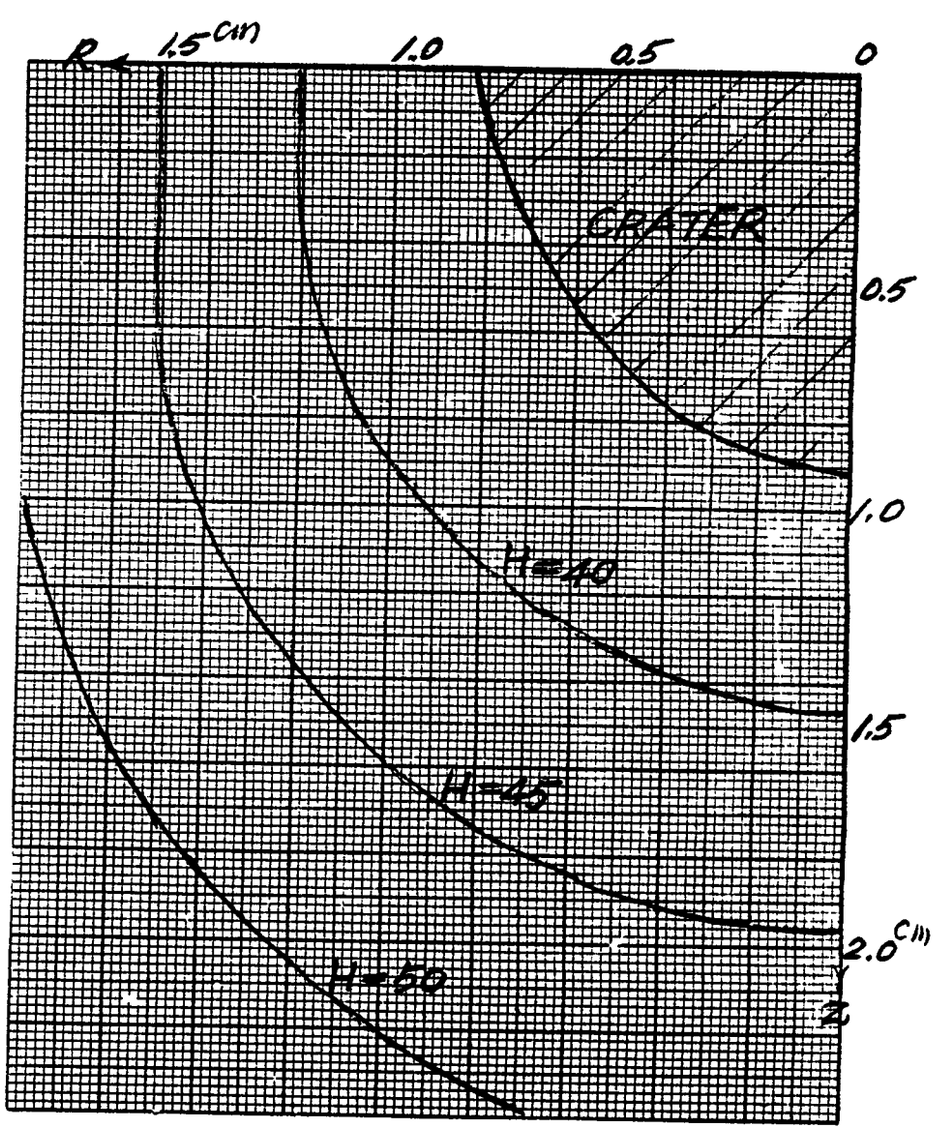

SUPPLEMENTARY

INFORMATION

AD-484 471 Johns Hopkins Univ., Baltimore, Md. Progress rept. no. 3, 1 Oct-31 Dec 65. 31 Dec 65 Contract DA-18-001- AMC-745(X)	No Foreign without approval of Aberdeen Proving Ground, Md.	No limitation	USAPG ltr, 10 Feb 69